CASE STUDY OF SMOKE SPREAD THROUGH ELEVATOR SHAFTS IN HIGH RISE BUILDINGS (REPORT OF 1ST PRIORITY SCENARIOS)

Qize He and Ofodike A. Ezekoye

UT Fire Research Group

Department of Mechanical Engineering

University of Texas at Austin

Abstract: The problem of smoke spread through elevator shafts in high rise buildings is analyzed theoretically and numerically in this report. Several comparisons are made in the report. For cases with no fire, theoretical calculations are performed for mass flow rates through elevator shafts when the flow is purely driven by differences between the interior temperature and external temperature (simple stack effect). These theoretical calculations consider cases in which the flow path includes either a tight building facade, or extreme ventilation (i.e., open building windows or open elevator doors). For cases with a fire, numerical simulations are performed for similar scenarios and a final comparison is made for moderate and cold weather conditions. Analysis shows that the stack effect for cold weather conditions produces comparable mass flow rates through the elevator shaft as a fire under moderate weather conditions. Not surprisingly, when simulations are performed with an enclosed elevator lobby, the additional flow resistance significantly delays smoke spread to the upper levels. When the doors on the enclosing walls are open, the gas temperature and pressure differences are almost 50% of the unenclosed conditions. We found that the ventilation condition on the fire floor has a major effect on both the total mass flow rate and also the smoke mass flow rate through the elevator shafts. For the relatively tight facade and limited ventilation cases, while the flow resistance is large creating a relatively smaller total mass flow rate, the smoke mass concentration is also large and these offset each other to create hazardous conditions on upper floors. The cold weather condition appears to enhance the fire hazard, but it is not the governing factor.

1 Introduction

The ICC is currently considering if it is necessary to require smoke transport mitigation for elevator lobbies and elevator shafts (hoistways) in high rise buildings. The current International Building Code (IBC) requires protection of elevator lobbies (or hoistway openings) when a building is a high rise, defined as having an occupied floor located more than 75 feet above fire department vehicle access. In order to rationally specify the required level of protection, the characteristics of smoke spread in high rise elevator shafts and impact of smoke penetration to the upper floors need to be better understood.

There has been greater attention placed on fires in high-rise buildings because of the 9/11/2001 disaster. Recent research on high rise fires have attempted to clarify the impact of the fire load on structural stability, human movement, and smoke transport [1,2]. Increasingly, simulation and theory are critical elements in these research studies. Smoke movement, in particular, is well suited to theoretical analysis. In high-rise fires, buoyancy forces can drive hot, toxic smoke gases to upper floors via vertical openings such as elevator shafts. As a result, a fire in the lower part of a high-rise building can cause smoke accumulation at the upper floors of the building. There are many historical cases in which this type of smoke transport has resulted in casualties [3].

The stack effect is also a consideration in tall buildings. The basic theoretical analysis of the stack effect in shafts is well known [3]. The pressure difference across the shaft can be related to the local temperature and elevation as

$$\Delta P = K_s \left(\frac{1}{T_0} - \frac{1}{T_l}\right) h, \tag{1}$$

where $K_s = 3460$ is a coefficient, T_0 and T_l are the environmental (exterior) temperature and local (interior) temperature, and h is the elevation. A network model was developed by Black [5,6] to predict the smoke movement in elevator shafts. In his model, one-dimensional and constant surface temperature assumptions were made. The fire was not directly modeled, but was assumed to affect the pressure and temperature fields. An improved zone model of smoke movement was developed by Cooper [7] and partially verified by salt-water experiments. These studies provide a general

understanding of the smoke transport through elevator shafts. Computational fluid dynamics (CFD) software is becoming a standard tool for fire hazard analysis and building fire safety design. It is useful to evaluate how CFD analysis can add value to our understanding of smoke transport processes in high rise buildings.

In this study, the stack effect caused by the temperature inside and outside the building is theoretically analyzed considering different vent areas along the flow paths. The CFD model Fire Dynamics Simulator (FDS), developed by the National Institute of Standards and Technology (NIST), was used to simulate a fire in a high rise office building. Factors including the ventilation condition of the upper layers, the operational condition of the sprinklers and the enclosure of the elevator lobbies are considered in affecting the smoke spread through elevator shafts. Although there are many ways that hot gas products from a fire can affect evacuees (e.g., gas toxicity, burns, etc.), research has shown that the safety threshold associated with visibility was usually the first to be reached in fires. Evacuees would more likely to refuse to move towards an exit when the visibility reduces below 10m. Thus we have summarized the safety time based on the visibility threshold as well as the mass flow rate at the fire floor at the end of the report.

2 Building models

2.1 The Building

This study was carried out based on a typical model of a high rise office building. The building geometry model was based on the layout of the Chicago Committee on High Rise Buildings' (CCHRB) Office Research Tower. It is a hypothetical building designed to be compliant with current building codes [e.g., mainly NFPA 101 (National Fire Protection Association 2012) and International Building Code 2012 (International Code Council 2012)]. This layout has already been adopted for research on high-rise building evacuation [13]. The entire building is 50 floors in height. The floor to floor height is 13 feet (about 4.0 m), except for the lobby at the ground level which has a floor to floor height of 39 feet (about 12.0 m). In order to improve the efficiency of the elevator operations, the office building is vertically divided into three elevator banks (low, middle and high). Different portions use different groups of elevators. For example, only the

lower passenger elevators are connected to the lower levels, while the elevators to upper floors don't have exits at these lower levels, as shown in Figure 1.

In high rise buildings, due to the stack effect, fire is potentially more dangerous when it occurs at the lower levels of the building. We considered a fire taking place in the office area at the first floor above the lobby since more combustible materials exist at this level than in the lobby. Thus, the regions directly connected to this level are the floors serviced by the lower level elevator banks

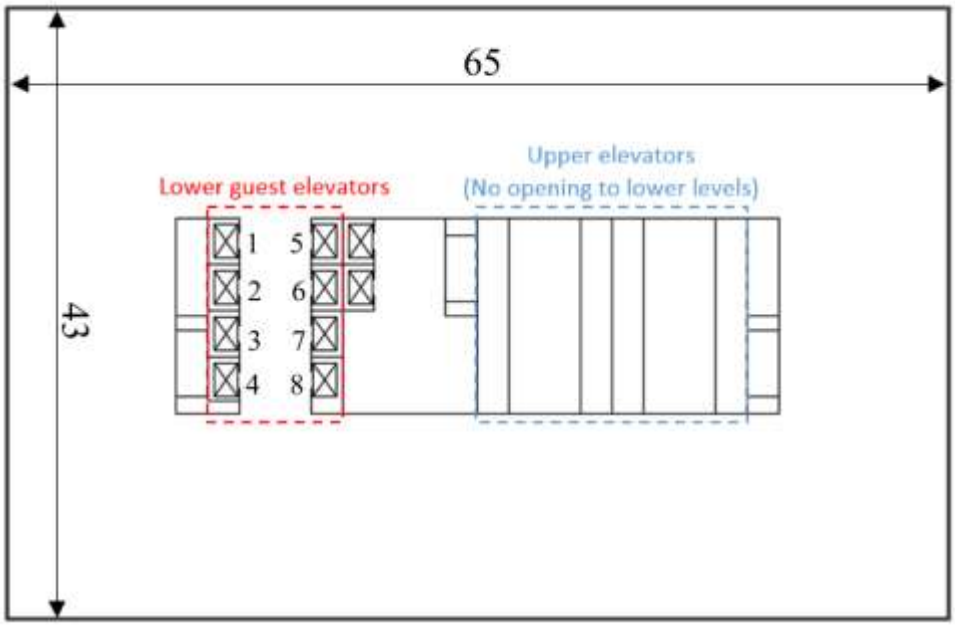

Figure 1 Plan view of low rise floors

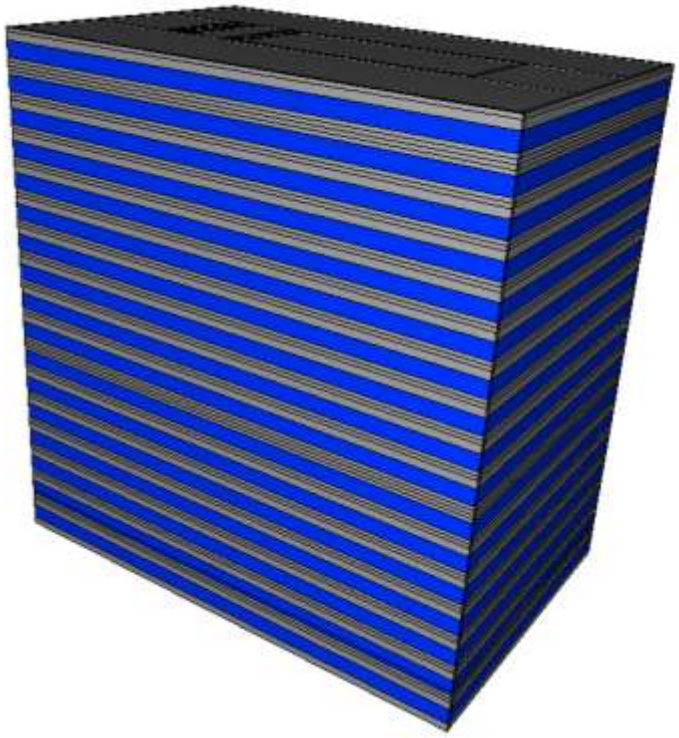

Figure 2 Building model

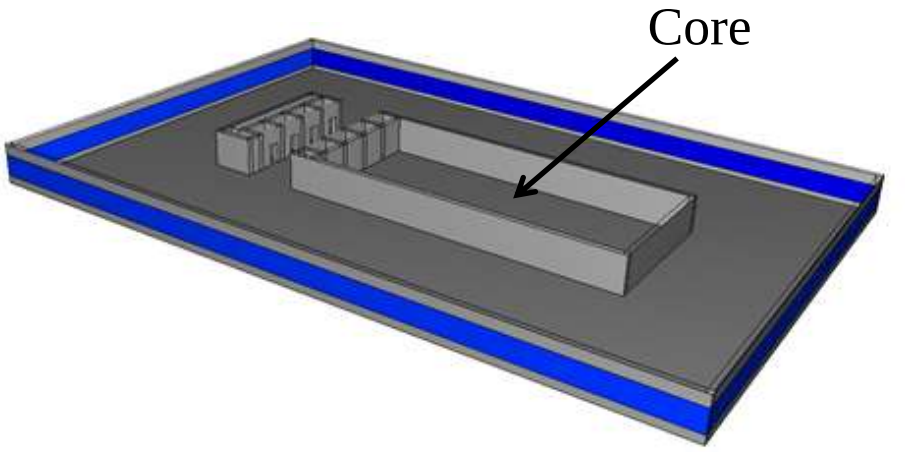

Figure 3 Internal structure of the upper levels

2.2 Building Flow Paths

Building flow paths consist of: (1) Leakages around the building envelope, (2) gaps around internal doors and elevator doors, (3) office area and vertical shafts, e.g., elevator

shafts and stair shaft. The general location of these flow paths are presented in Fig.4. Note that the shapes and areas of flow path may vary from building to building, and more than one vertical shafts and internal doors may exist along the paths.

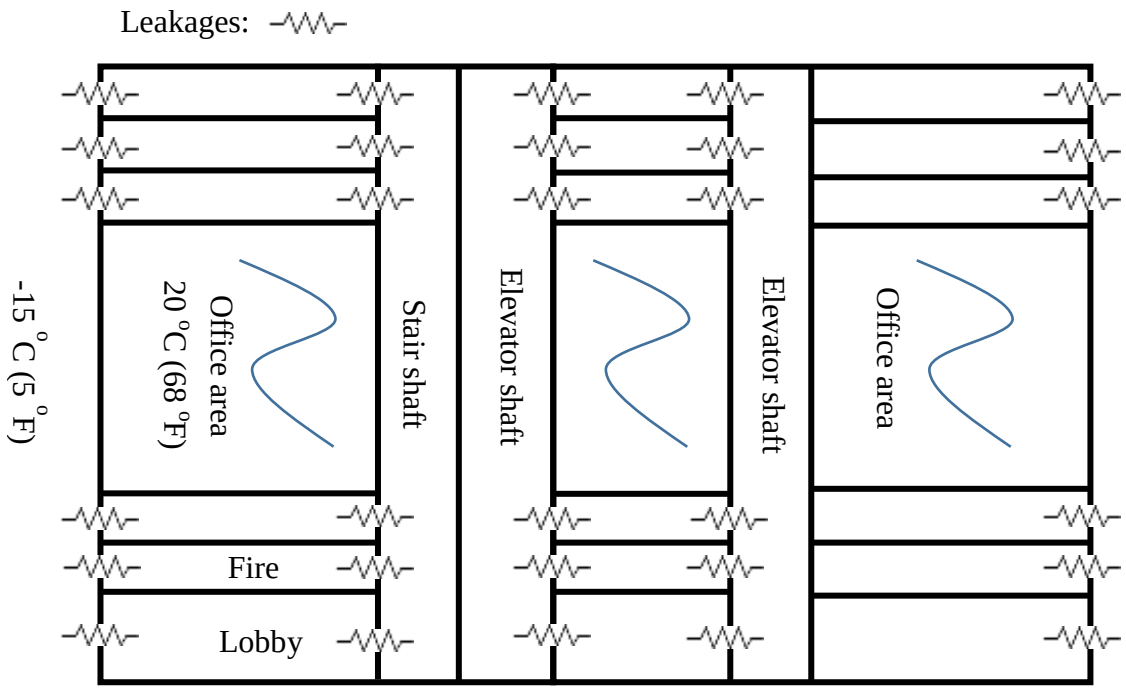

Figure 4 Flow paths and environmental and local temperatures for a cold weather case

Among them, the most important flow paths affecting the smoke spread through elevator shafts to other levels are the gaps around elevator doors. In Klote's research [5], an area of roughly 0.047m^2 for elevator door leakage was given. We surveyed the leakage area of an actual passenger elevator door and stair door in a typical office building as shown in Fig. 5. The dimension of the elevator door is 42 inches by 84 inches. Gaps are not only found at the centerline of the door, but also along the edges. The width of the gaps is approximately 3/16 inch as shown in Fig. 4. Thus the total area of the gaps is about 63.0 square inches (0.041m^2). This value is very close to the leakage area used in Klote's research. As a conservative consideration, 0.05m^2 is used as the leakage area of a single elevator door in this research.

The stair door is better sealed than the elevator door. Due to the existence of the gate groove, there is hardly a gap around the stair door except for the bottom frame. Generally

the leakage through stair doors is much smaller than through elevator doors. As a simplification, the smoke spread is assumed to occur only through the elevator shafts in this study.

The other sizes of the flow paths refer to the recommended values in the NFPA standard for smoke control systems. The values listed in Table 1 are representative leakage areas that commonly exist in office buildings and are deemed sufficient for our characterizing the smoke spread characteristics [17,18].

Figure 5 Leakage area locations of a typical passage elevator door (left) and stair door (right) in office buildings

The elevator cars in the shafts might have significant effect on the smoke spread in the building. The presence of the cars would reduce the sectional area of the shafts and would likely delay the smoke spread rate. According to the current codes, the elevators are not typically allowed to be used in case of fires. All the cars should be recalled to the ground floor during a fire which has activated a detector in the elevator lobby. In this study, the elevator shafts were simplified and modeled as being empty. This situation may also be regarded as moving all the elevator cars to the lobby floor.

There also have to be leakages at the building envelope. According to the ASHRAE Handbook, the leakage area of the exterior walls is about 0.002 in^2/ft^2, and the flow coefficient is about 0.65. Thus, the calculated leakage area of the exterior walls per floor is $A_w = 4 \times 2 \times (63 + 43) \times 0.00014 = 0.12m^2$ for the upper floors, and $A_w = 12 \times 2 \times (63 + 43) \times 0.00014 = 0.36m^2$ for the lobby floor. The exterior leakage area of any given floor of the building is quite small, which indicates that most of the buildings are well-enclosed nowadays.

Table 1 Summary of flow paths

Component	**Area (m^2)**	**Reference**
Exterior wall of upper layers	0.12	
Exterior wall of lobby	0.36	
Open window	Perimeter×2 (2m in height)	-
Interior single door	1.9	[17,18]
Interior double door	3.9	[17,18]
Closed interior single door	0.016	[17,18]
Closed interior double door	0.027	[17,18]
Open elevator door	2.0	-
Closed elevator door	0.05	[5]

2.3 Flow Loss Coefficient

According to the ASHRAE Handbook[18], tests have been done to evaluate the leakage mass flow through doors as shown in Figure 6. Their results were carried out for a pressure difference of 0.3 inches of water (about 74.8Pa). We calculated a flow loss coefficient, *K=3.56*, and a discharge coefficient, $C_D = 0.53$, valid for crack widths from 0 to 0.3 inches. For the exterior leakages at the building envelope, a discharge coefficient, $C_D = 0.65$, was used according to ASHRAE Handbook[18].

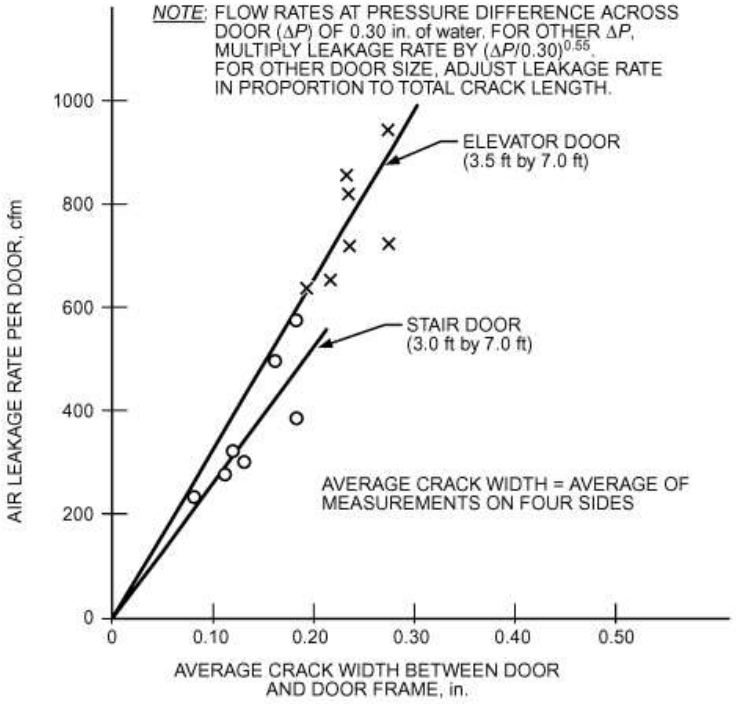

Figure 6 Mass flow rate varies with crack width, from ASHRAE Handbook[18]

3 Scenario analysis

This study considered a heat and mass transfer problem with the combination of stack effect and fire. A number of factors influence the smoke spread within this building including the environmental temperature, the leakage area along the flow paths, the location of the fire and its heat release rate (HRR). As first priority scenario, fire was located at the second floor (first level above the lobby). Thus, the configuration of doors and windows at this level are critical. The elevator doors on the fire level are either closed or open. We also considered different ventilation situations for the building. The scenarios we considered are summarized in Table 2. New scenarios are welcome as next steps.

Table 2 Summary of Fire Scenarios

Category	Case	Weather	Elevator door of fire level	Envelope of fire level	Envelope of other levels	Sprinkler	Elevator lobby	Method
Stack effect without fire	SE-1	Cold (5^{o}F)	Leakage	Leakage	Leakage	-	Unenclosed	Theoretical
	SE-2	Cold (5^{o}F)	Leakage	Open	Leakage	-	Unenclosed	Theoretical
	SE-3	Cold (5^{o}F)	Leakage	Open	Open	-	Unenclosed	Theoretical
	SE-4	Cold (5^{o}F)	Open	Leakage	Leakage	-	Unenclosed	Theoretical
	SE-5	Cold (5^{o}F)	Open	Open	Leakage	-	Unenclosed	Theoretical
	SE-6	Cold (5^{o}F)	Open	Open	Open	-	Unenclosed	Theoretical
Fire with open elevator door	FO-1	Warm (68^{o}F)	Open	Open	Closed	Failed	Unenclosed	FDS
	FO-2	Warm (68^{o}F)	Open	Open	Open	Failed	Unenclosed	FDS
	FO-3	Warm (68^{o}F)	Open	Open	Open	Activated	Unenclosed	FDS
	FO-4	Warm (68^{o}F)	Open	Open	Open	Failed	Enclosed with open door	FDS
	FO-5	Warm (68^{o}F)	Open	Open	Open	Activated	Enclosed with open door	FDS
	FO-6	Warm (68^{o}F)	Open	Open	Open	Failed	Enclosed with leakage	FDS
Fire with closed elevator door	FC-1	Warm (68^{o}F)	Leakage	Leakage	Leakage	Failed	Unenclosed	FDS
Combination of fire and stack effect	FC-2	Cold (5^{o}F)	Leakage	Leakage	Leakage	Failed	Unenclosed	FDS

4 Theoretical analysis of the stack effect without fires

The stack effect without the effect of fire was first studied. Cold weather outside the building was considered to enhance the stack effect within the building. The outside temperature was considered to be -15 ^{o}C (5 ^{o}F) while the inside temperature remains 20^{o}C (68 ^{o}F) by the heating system. When considering the total 18 floors of the low rise (80m), the pressure difference within the building caused by the temperature difference can be calculated by Eq.(1).

$$\Delta P = K_s \left(\frac{1}{T_0} - \frac{1}{T_l}\right) h = 3460 \times \left(\frac{1}{258} - \frac{1}{293}\right) \times 80 = 128\ Pa \qquad (2)$$

This is the maximum pressure difference from top to the bottom. To obtain the neutral plane height and the mass flow through these leakages, the detailed flow paths must be specified. The leakage areas are summarized in Table 3. The Flow Loss Coefficient was addressed in Section 2.3.

Table 3 Leakage parameters

Case	Elevator door of fire floor	Elevator door of other floors	Exterior leakage of fire floor	Exterior leakage of lobby	Exterior leakage of other floors
SE-1	0.05 m^2	0.05 m^2	0.12 m^2	0.36 m^2	0.12 m^2
SE-2	0.05 m^2	0.05 m^2	212 m^2	0.36 m^2	0.12 m^2
SE-3	0.05 m^2	0.05 m^2	212 m^2	212 m^2	212 m^2
SE-4	2.0 m^2	0.05 m^2	0.12 m^2	0.36 m^2	0.12 m^2
SE-5	2.0 m^2	0.05 m^2	212 m^2	0.36 m^2	0.12 m^2
SE-6	2.0 m^2	0.05 m^2	212 m^2	212 m^2	212 m^2

There are two flow resistance paths between the elevator shaft and outer space as shown in Fig.23. For upper floors, the general flow resistance can be calculated as Eq.(3).

$$\frac{1}{C_d A} = \sqrt{\frac{1}{(8C_{d,e}A_e)^2} + \frac{1}{(C_{d,w}A_w)^2}} \qquad (3)$$

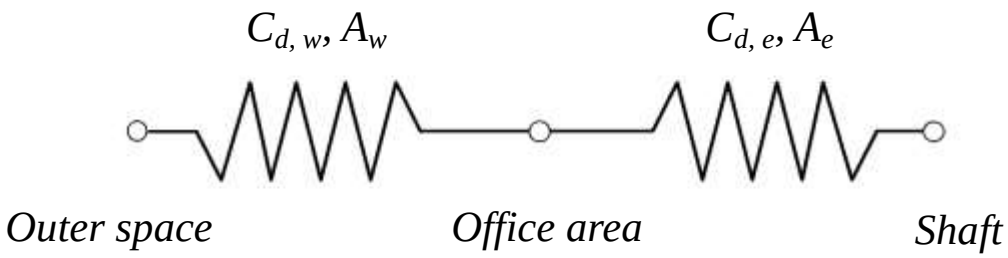

Figure 7 Combination of the flow resistance

Table 4 Leakage Parameters

Case	General Flow Resistance C_dA / m^2		
	Fire Floor	**Lobby level**	**Other Floors**
SE-1	0.073662	0.161812	0.073662
SE-2	0.224	0.161812	0.073662
SE-3	0.224	0.224	0.224
SE-4	0.077999	0.161812	0.073662
SE-5	12.77673	0.161812	0.073662
SE-6	12.77673	0.224	0.224

The pressure difference can then be calculated by Eq.(1). The mass flow rate, $\dot{m}$, at the openings is a function of the pressure difference, Δp, as shown in Eq.(4)

$$\dot{m} = C_D A\sqrt{2\rho\Delta p}. \tag{4}$$

where A is the area of the leakage. Using the mass balance, the total inflow rate should equal the total outflow rate.

$$\sum \dot{m}_{in} = \sum \dot{m}_{out} \tag{5}$$

Then, the height of neutral plane H_{np} can be calculated as shown in Table 5. The mass flow rate through the fire floor is also presented. If fire had occurred and produced ambient temperature smoke, the smoke would be carried by this mass flow into the elevator lobby. We find that when all the doors and windows on the fire floor are closed, the mass flow rate caused by the stack effect is relatively small compared to the open door and/or window cases.

The pressure difference of these cases as functions of floorheight are also presented in Figure 8. These computed stack effect pressure differences are of similar magnitude as those reported in the research of Jo[19].

When the elevator doors and windows at the fire level are all opened, the neutral plane height is much lower than the closed door/window cases, while the mass flow rate at fire level is significantly larger.

Table 5 Neutral Plane Height and Mass Flow Rate at Fire Floor

Case	Neutral Plane Height H_{np}	Total Mass Flow Rate at Fire Floor	Mass Flow Rate at Fire Floor per Shaft
SE-1	41.7 m	0.767 kg/s	0.096 kg/s
SE-2	38.2 m	2.170 kg/s	0.271 kg/s
SE-3	43.9 m	2.412 kg/s	0.302 kg/s
SE-4	40.2 m	2.262 kg/s	0.283 kg/s
SE-5	14.3 m	12.582 kg/s	1.5728 kg/s
SE-6	16.2 m	37.068 kg/s	4.634 kg/s

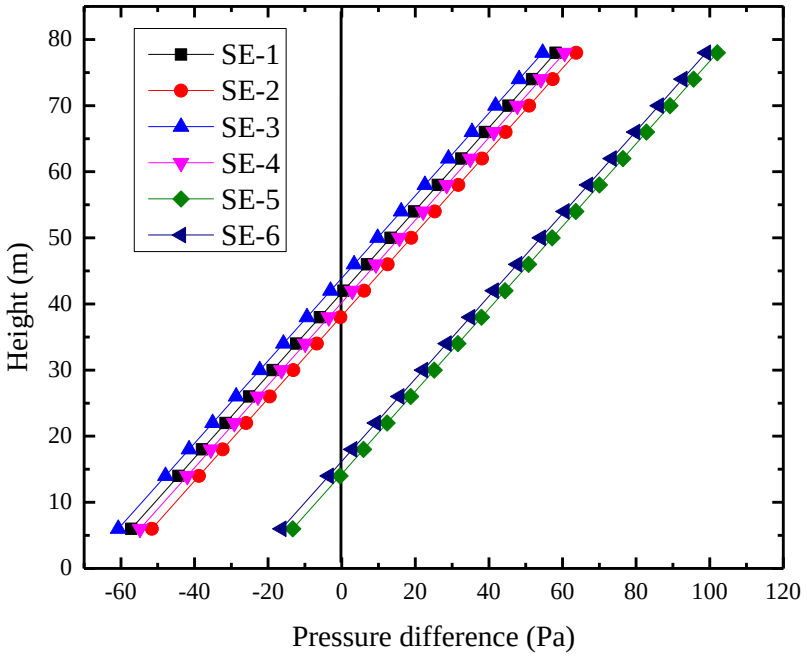

Figure 8 Pressure difference caused by the stack effect (Cold weather)

5 Mathematical Approach of CFD simulation

5.1 Flow Model

The FDS model numerically solves approximate forms of the Navier-Stokes equations [8,9]. The equations for large-eddy simulation (LES) modeling of Navier-Stokes are derived by separating turbulent motions into large and small eddies by a filter. Then any flow variable, $\varphi(x,t)$, can be decomposed by filtering it into a resolved large-scale component, $\varphi_L(x,t)$, and a sub grid-scale component, $\varphi'(x,t)$, as

$$\varphi(x,t) = \varphi_L(x,t) + \varphi'(x,t). \tag{6}$$

The large-scale component is simulated directly, while small eddies are modelled by means of the Smagorinsky form of LES.

Another important assumption is based on work by Rehm and Baum[10] that for low speed applications like fire, the pressure, $p(x,y,z,t)$, can be decomposed into a "background" pressure, $\bar{p}(z,t)$, and a perturbation, $\tilde{p}(x,y,z,t)$. The background pressure satisfies the thermodynamic constraints and is expressed in the ideal gas law,

$$p(x,y,z,t) = \rho TR \sum_\alpha \frac{Z_\alpha}{W_\alpha} + \tilde{p}(x,y,z,t). \tag{7}$$

Here, Z_α and W_α are the mass fraction and molecular weight of the gaseous species α. This is appropriate for low-speed, thermally-driven flows with an emphasis on smoke and heat transport from fires. FDS also considers the stratification of the atmosphere as

$$\frac{dp_0(z)}{dz} = \rho_0(z)g \ . \tag{8}$$

5.2 Combustion Model

A mixing-limited, infinitely fast reaction combustion model is used. The reactant species in any given grid cell are converted to product species at a rate determined by a characteristic mixing time. The heat release rate per unit volume is defined by summing the product of all the species mass production rates and their respective heats of formation

$$\dot{q}''' = -\sum_\alpha \dot{m}'''_\alpha \Delta h_{f,\alpha}. \tag{9}$$

5.3 HVAC Model

A HVAC (Heating, Ventilation, and Air Conditioning) submodel is available in FDS to simulate the gas flow through small leakages. The HVAC solver uses simple conservation equations of mass and energy combined with an implicit solver for the momentum conservation equation based on the MELCOR solver [11]. It does not account for mass storage within the gas transport route. The conservation equations of mass, energy, and momentum of species *j* are

$$\sum_j \rho_j u_j A_j = 0 \ , \tag{10}$$

$$\sum_j \rho_j u_j A_j h_j = 0 \ , \tag{11}$$

$$\rho_j L \frac{du_j}{dt} = (p_{in} - p_{out}) + (\rho g \Delta z)_j - \frac{1}{2} K_j \rho_j |u_j| u_j, \tag{12}$$

where L is the length of the duct segment, and K is the loss coefficient of the duct segment. The measured minor loss is usually given as a ratio of the head loss $h_m = \Delta p/(\rho g)$ through the constriction to the velocity head $v^2/(2g)$ of the associated piping system. Thus, the coefficient can be defined by Equation (13).

$$K = \frac{h_m}{v^2/(2g)} = \frac{\Delta p}{\frac{1}{2}\rho v^2} \tag{13}$$

This minor loss coefficient is related to the discharge coefficient, C_d, through the equation:

$$K = \frac{1}{{C_d}^2} \tag{14}$$

5.4 Water Suppression Model

A water suppression model, also available in FDS, is applied in these simulations. It is assumed that water impinging on the fuel surface takes energy away from the pyrolysis process and thereby reduces the burning rate of the fuel. An empirical way to account for fire suppression by water is to characterize the reduction of the pyrolysis rate in terms of an exponential function. The local mass loss rate of the fuel is expressed in the form

$$\dot{m}_f{}''(t) = \dot{m}_{f,0}{}''(t) e^{-\int k(t) dt} \tag{15}$$

Here $\dot{m}_{f,0}''(t)$ is the user-specified burning rate per unit area when no water is applied and k is a function of the local and instantaneous water mass per unit area, m_w'', expressed in units of kg/m^2.

$$k(t) = E\_COEFFICIENT \times m_w'' \tag{16}$$

The parameter E_COEFFICIENT must be obtained experimentally, and it is expressed in units of m^2/(kg·s). Experiments of water suppression of rack-storage commodity fires conducted by NIST show that the E_COEFFICIENT is nearly 1.0[12].

5.5 The Mesh

Considering the large length scales of the physical/computational domain (i.e., 70 m × 45 m × 72 m) a relatively coarse mesh size of 0.5m was used. The total number of grid cells is 1,866,240 which were divided into 8 meshes for parallel computing.

6 Design of fire

6.1 The Heat release rate

As previously noted, after 9/11/2001, fires in office high rise buildings have been extensively investigated. The most common fire scenario in an office building is the office workstation fire. Full scale fire testing of a single office workstation has been carried out by NIST as part of the 9/11 investigation[14]. They found that the peak heat release rate (HRR) for a single workstation was about 7.0 MW with a relative expanded uncertainty of approximately $\pm$15%. The t-squared fire model was adopted to describe the fire growth phase [15].

$$\dot{Q} = \alpha t^2 \tag{17}$$

Here, $\dot{Q}$ is the transient heat release rate (HRR) of the fire of the fire, α is the fire growth rate in units of *kW/s*^{2}, and t is the time from ignition. Since the furniture contains a large amount of foam material, the fast t-squared growth model is used for the early stage (growth phase) burning process based on fire test data for similar material[3]. According to NFPA 204M (National Fire Protection Association 1985), the fast fire growth rate of $\alpha = 0.0469\ \mathrm{kW/s^2}$ is suitable for this scenario. Thus, the calculated

duration of the fire growth phase is 386s. Figure 9 presents the designed heat release rate (HRR) profile under well-ventilated conditions.

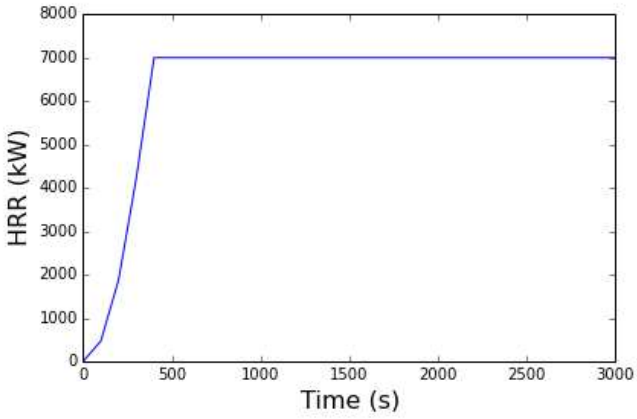

Figure 9 Heat release rate (HRR) of fire under well-ventilated conditions

7 FDS simulation with open elevator doors

The main objective of this study was to evaluate the necessity of enclosing the elevator lobby under fires, while varying other factors (e.g., the ventilation condition of the upper floors and the status of sprinklers). Table 2 summarizes the fire scenarios simulated in this study. In this section (7), we evaluate extremes in the ventilation conditions while keeping the interior and environmental temperatures fixed at 20 C (68F). In the following section (8), we will fix the ventilation condition using only the building envelope leakage and consider extremes in the interior versus environmental temperatures.

Table 6 Summary of Fire Scenarios

Case	Fire Location	Peak HRR	Windows	Sprinkler	Elevator lobby
FO-1	First story above lobby	7MW	Closed	Failed	Unenclosed
FO-2	First story above lobby	7MW	Open	Failed	Unenclosed
FO-3	First story above lobby	7MW	Open	Activated	Unenclosed
FO-4	First story above lobby	7MW	Open	Failed	Enclosed with open door
FO-5	First story above lobby	7MW	Open	Activated	Enclosed with open door
FO-6	First story above lobby	7MW	Open	Failed	Enclosed with leakage

7.1 Ventilation Effects on Upper Floors

Because the interior and environmental temperatures are initially the same, smoke spreads through the elevator shafts due to the fire stack effect which is caused by the pressure difference between the hot column of gas in the elevator shaft and the cooler gases on any given floor. It is important to determine whether the gas pressure in the upper floors changes because of the fire. The windows of most high rise buildings are closed for both safety and energy savings objectives. If the upper floors are absolutely enclosed and the gas temperature is slightly heated by the fire, the gas pressure of the upper floors will increase. Further, under such a condition, the upper floor pressure is less coupled to the temperature outside of the building (i.e., the ambient temperature). In reality, the HVAC system in the building would couple pressure and flow at different floors and a somewhat more complex scenario would occur. Two extreme ventilation conditions for the upper floors were considered and compared. FO-1 was the ideally enclosed upper floor scenario with all the windows closed on the upper floors. For FO-2, the windows on the upper floors were assumed to be opened thus connecting the upper floor office areas to the ambient conditions. The second scenario, while generally not likely, represents a more significant hazard.

Figure 10 presents the comparison of the pressure distribution for both cases. The pressure increases significantly within the elevator shafts in both conditions because of the fire gases. When the upper floor windows are intact, the pressure in the open space of the upper floors also increases slightly. The pressure would remain zero (i.e., be the same as the ambient pressure) if the windows of the upper floors are open. Figure 11 also shows the pressure changes inside and outside the elevator shaft when the upper floor windows are closed. Both the pressure inside and outside the elevator shaft increase with elevation, and the pressure generally becomes steady after 1000s. Note that the scale is significantly different between figure 11a and 11b.

The pressure difference between the space inside and outside the shaft generates the gas flow throughout the elevator shafts which carries the combustion products to the upper floors.

Figure 12 presents the comparison of the nearly steady state pressure change with elevation inside and outside of the shaft for both cases of windows closed and open. Interestingly, their inside pressures are similar but the pressures on each floor are larger for the case in which the upper floor windows are closed. As a result, the maximum pressure difference across the shaft is about 12 Pa when the windows are closed, while it is about 16 Pa when the windows are open. According to the Eq. (12), the mass flow rate is the square root of the pressure difference. Thus, the effect of window ventilation on upper floor smoke transport is about a 15% increase in mass flow rate. This is acceptable considering the uncertainty of other factors (e.g., fire size, fire location, material properties, etc.). As a simplification, the windows in future simulations are considered to be open to keep the zero pressure on the upper floor spaces.

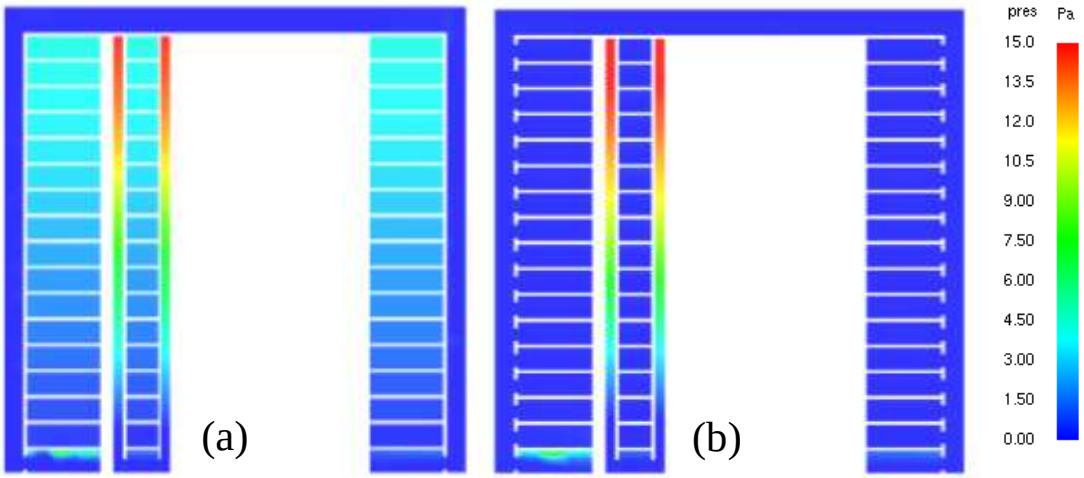

Figure 10 Pressure contour plot at section Y=20.5m at 3000s: (a) windows closed; (b) windows open

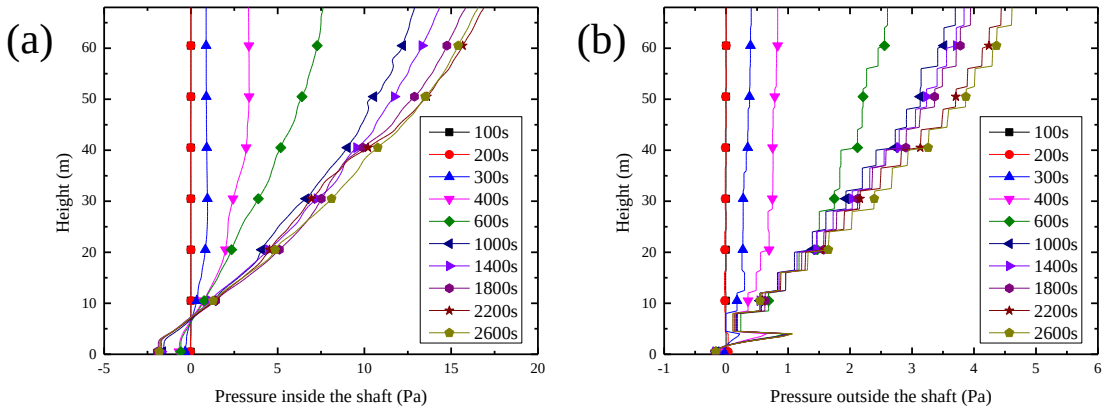

Figure 11 Pressure inside and outside the shaft with upper floor windows closed: (a) Inside the shaft; (b) Outside the shaft

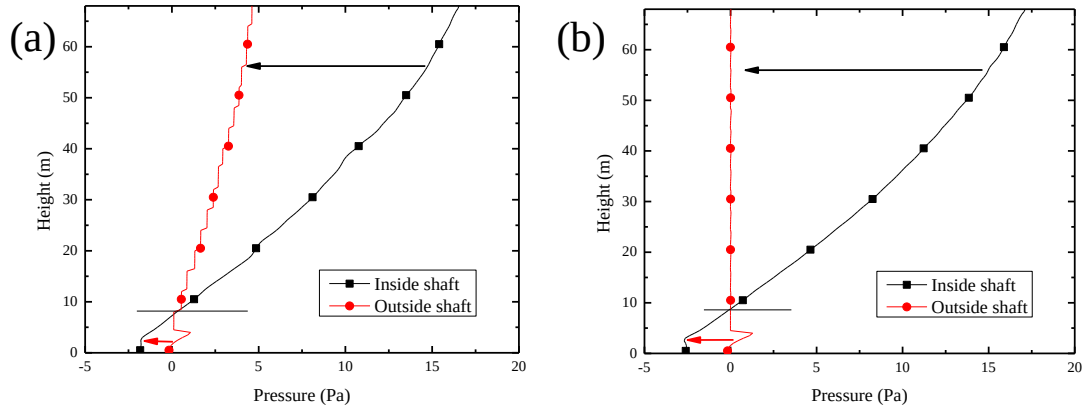

Figure 12 Pressure inside and outside the shaft at 3000s: (a) windows closed; (b) windows open

7.2 Sprinkler effect

As required by building codes, sprinklers should be installed in these high rise office buildings to meet fire protection objectives. Commonly used closed sprinklers are pre-pressurized and can be activated when the sprinkler reaches a predetermined temperature.

Quick Response (QR) fire sprinklers are incorporated into this model. Four sprinklers are installed with a spacing of 5.0m at an elevation of 3.5m above the fire area as shown in Fig.13. Table 7 summarizes the parameters assigned to the sprinklers.

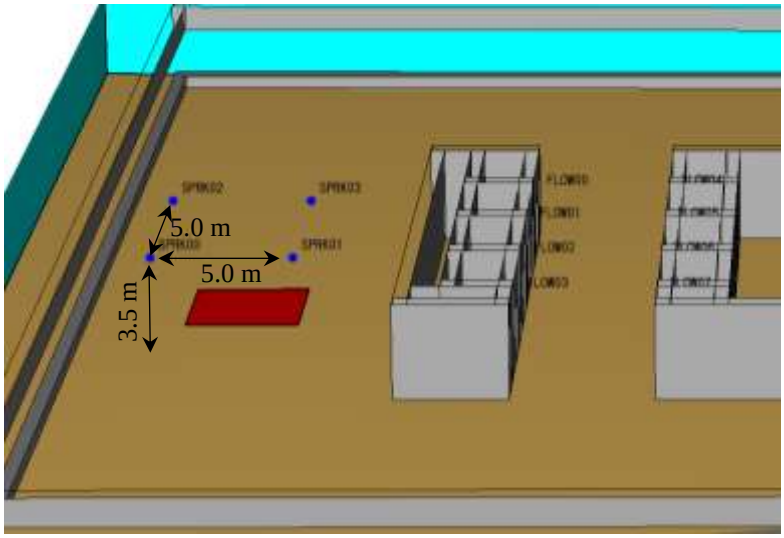

Figure 13 Location of the sprinklers

Table 7 Parameters of fire sprinklers

ID	Attribute
Activation Temperature	74°C (165 F)
Response Time Index RTI	148 $m^{1/2}s^{1/2}$
C Factor	0.7 $m^{1/2}$ / $s^{1/2}$
Flow Rate	189.3 L/min
Particle Velocity	10.0 m/s

Figure 14 presents the temperature of the sprinklers along with time after ignition for the configuration described above. The temperature of the sprinklers increases quickly due to the fire and exceeds the activation temperature at about 300s. At this time, the sprinklers are activated, and their temperatures quickly drop.

The activation of the sprinklers soon extinguishes the fire. Figure 15 presents the heat release rate (HRR) of fires with and without the presence of the sprinklers. When the sprinklers are activated, the HRR of the fire quickly drops to zero. Note that the HRR evolution for the sprinklered cases is driven by the suppression model detailed in section 2.3.

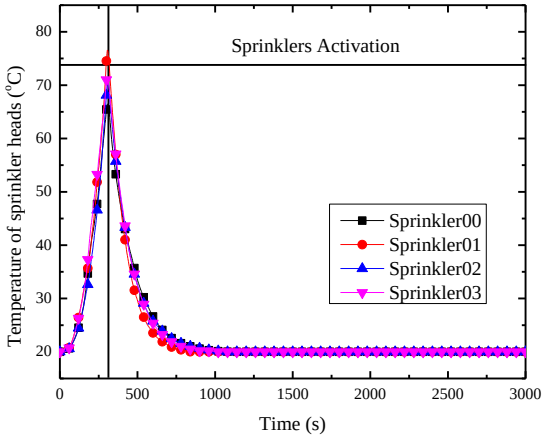

Figure 14 Temperature of the sprinklers

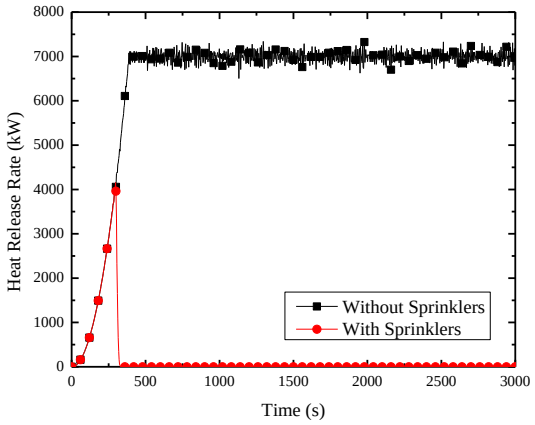

Figure 15 Heat release rate (HRR) with and without the sprinklers

Even when the fire is extinguished, the gas temperature within the building has already been elevated. Thus the stack effect continues to exist in the shafts, driving the smoke sequentially to the upper floors. Figures 16 and 17 present the smoke spread process without and with the effect of the sprinklers. When the sprinklers fail (i.e., are not activated), the smoke generated from the fire continually fills the fire floor. The smoke then starts to affect the elevator shaft at about 200s. The smoke continues rising inside the elevator shaft and completely fills the shaft at about 500s. Meanwhile, smoke flows into the other floors through the small leakage areas around the elevator doors. When the sprinklers are activated at about 300s, the fire is suppressed, but smoke still gathers on the fire floor. Then, the smoke gradually migrates to the upper floors. Compared with the

situation without sprinklers, the smoke density of both the upper and lower floors is much lower.

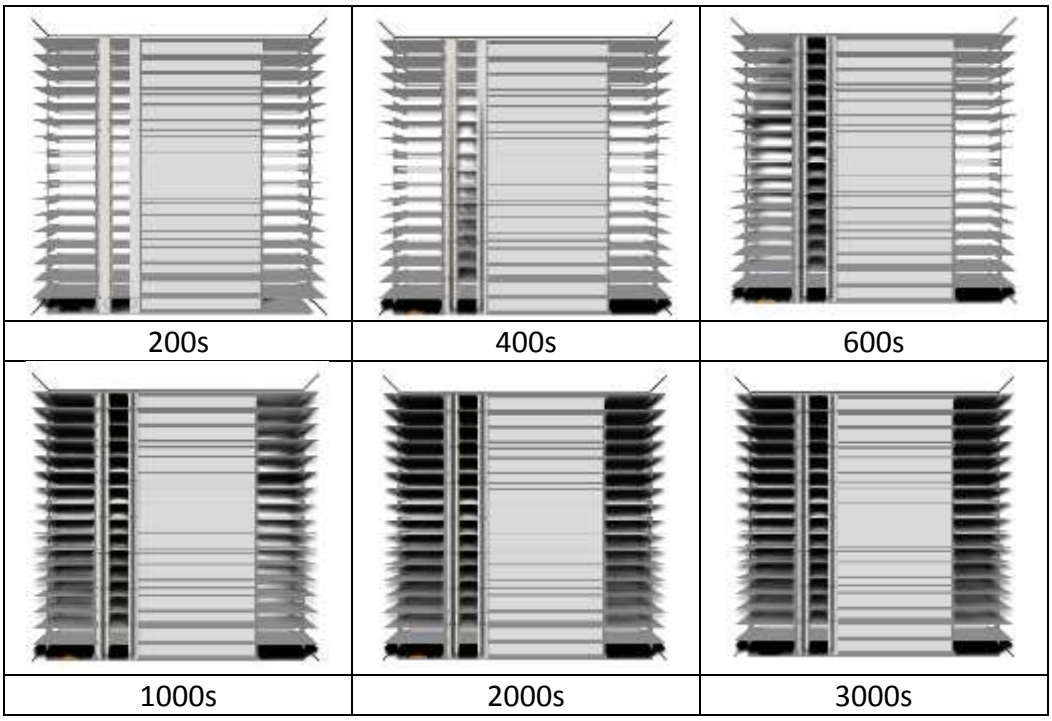

Figure 16 Smoke spread visualization of FO-2 (without sprinklers)

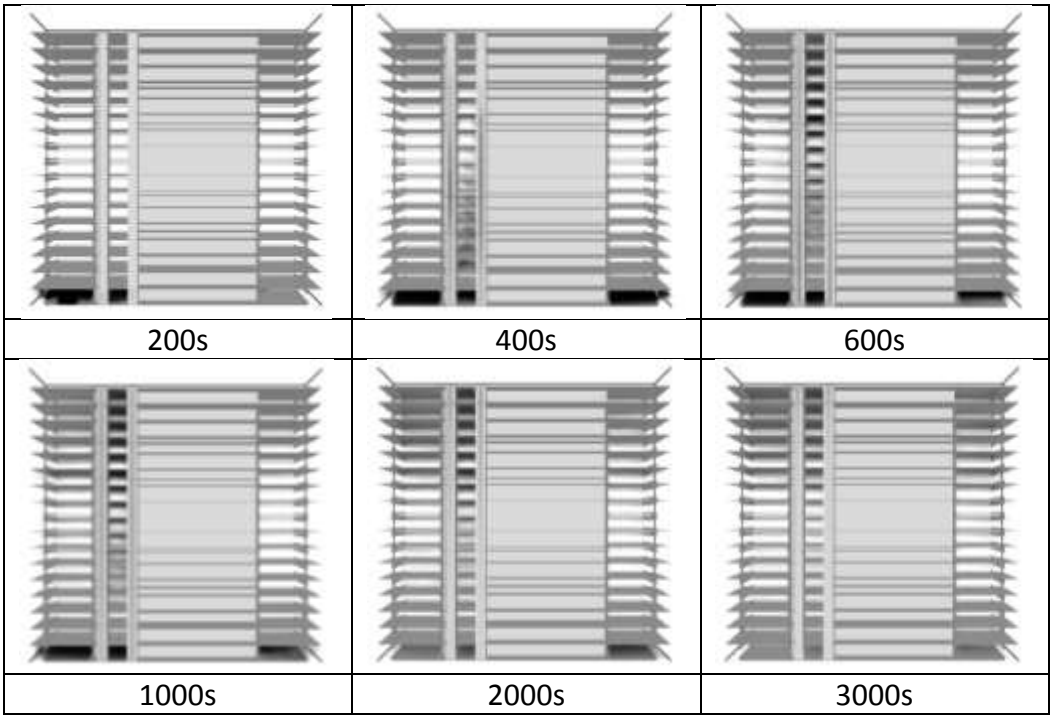

Figure 17 Smoke spread visualization of FO-3 (with sprinklers)

Figure 18 presents the temperature distribution in the elevator shaft for the cases without and with the effects of sprinklers. When the sprinklers do not operate, the temperature distribution gradually becomes steady at about 500s. Due to heat losses to the elevator shaft walls, the final gas temperature decreases with elevation. However, when the sprinklers operate, the temperature of the first floor above the lobby quickly cools, and temperature profiles reverses. The gas temperature at the fire floor could even be slightly lower than the initial air temperature due to the evaporation of the water drops from the nozzles.

Similar results are found for the pressure difference across the elevator shafts. Figure 19 presents the pressure difference distribution of the cases without and with the effects of sprinklers. Without the effect of the sprinklers, the pressure difference gradually becomes steady which increases with elevation. However, when the sprinkler operates, the pressure difference gradually decreases, and becomes nearly zero after 1400s. This indicates the stack effect in the elevator shaft becomes weaker after fire extinction.

The decrease of the pressure difference results in a reduction of the mass flow rate through the elevator shafts. Figure 20 presents a comparison of the mass flow rate through one elevator shaft, without and with the effect of sprinklers. The mass flow rate decreases immediately after the extinction of the fire.

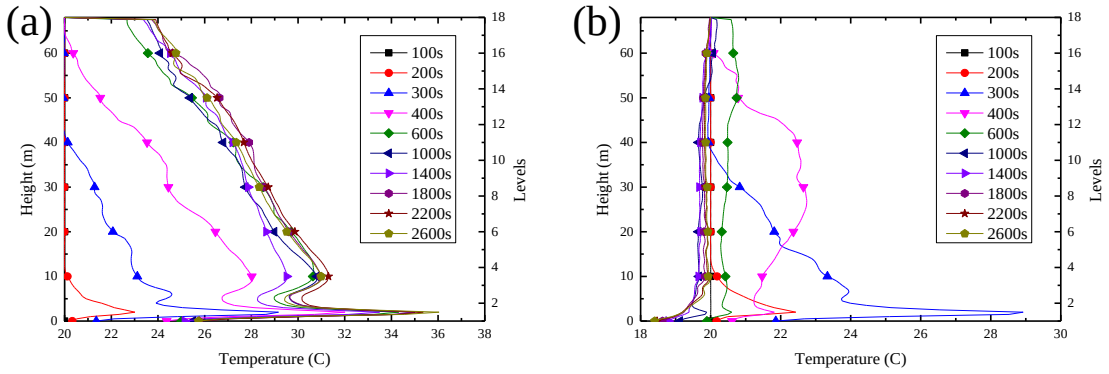

Figure 18 Temperature distribution in the elevator shaft: (a) FO-2 (without sprinklers); (b) FO-3 (with sprinklers)

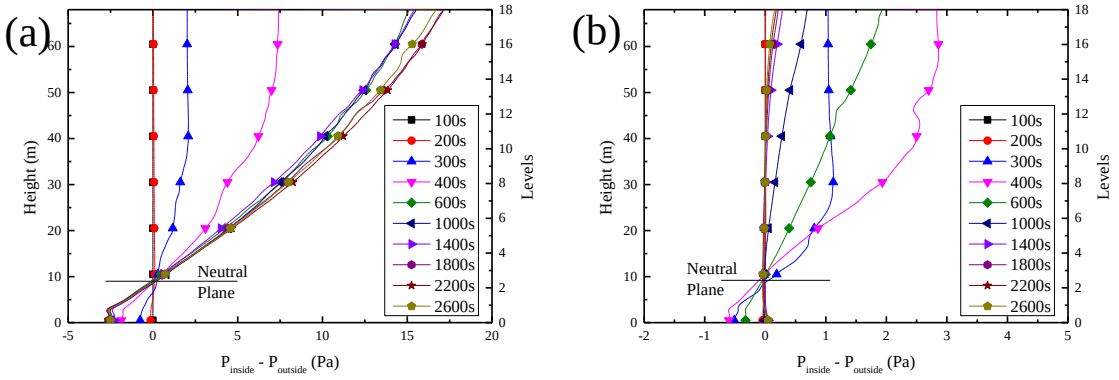

Figure 19 Pressure distribution in elevator shaft: (a) FO-2 (without sprinklers); (b) FO-3 (with sprinklers)

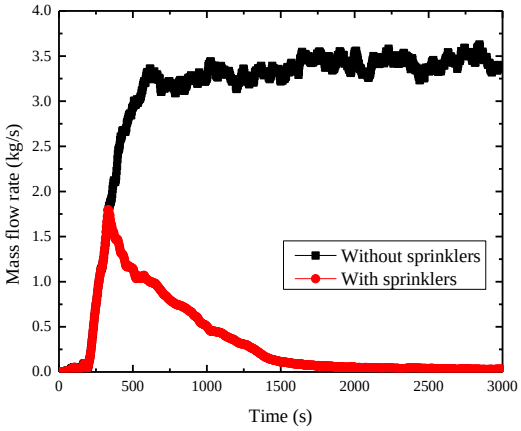

Figure 20 Mass flow rate through the elevator door (Elevator 3) at fire level.

7.3 Enclosure of the elevator lobbies

The effectiveness of enclosing the elevator lobbies was also considered in this study. Even when the lobbies are enclosed, there are still doors on the enclosing walls to access the lobbies. These doors might either be open or closed. We considered the open door condition in FO-4 and the condition of closed door with small leakage areas in FO-6. These results are also compared with the unenclosed condition in FO-2. The enclosing conditions of the elevator lobbies are depicted in Fig. 21.

Figures 22 and 23 present the general smoke spread rate when the elevator lobbies were enclosed. Compared with the unenclosed cases, the presence of the enclosure (no matter whether the door is open or closed) significantly delays the smoke spread. When the doors are open, the smoke started to affect the elevator shaft at about 600s, and it took another 300s for the smoke to fill the shaft. Significant smoke still gathers at the upper levels. However, when the doors are closed, very little smoke penetrates into the elevator lobby on the fire level. There is hardly any smoke at the upper levels during the whole simulation.

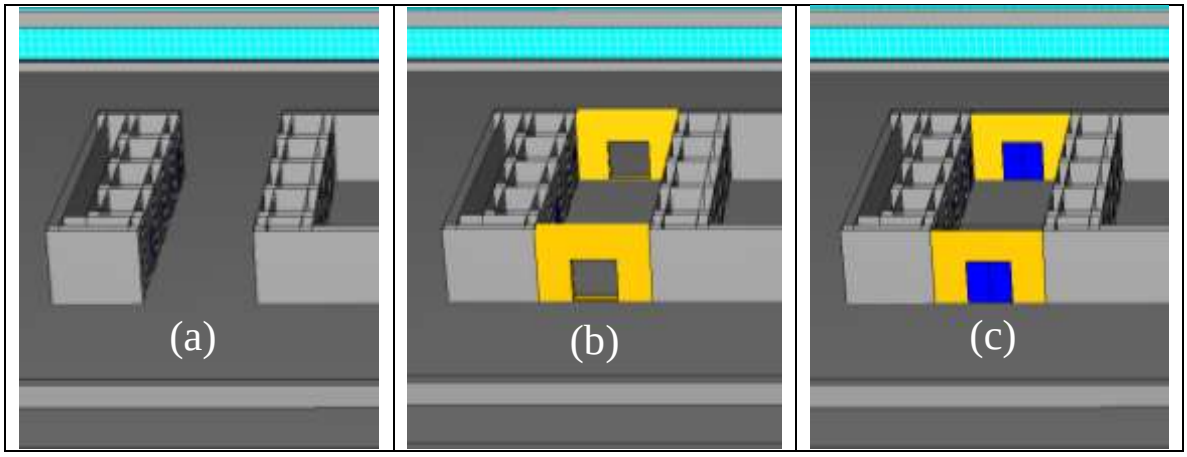

Figure 21 Structure of the elevator lobby: (a) FO-2 (unenclosed); (b) FO-4 (enclosed with open doors); (c) FO-6 (enclosed with leakages)

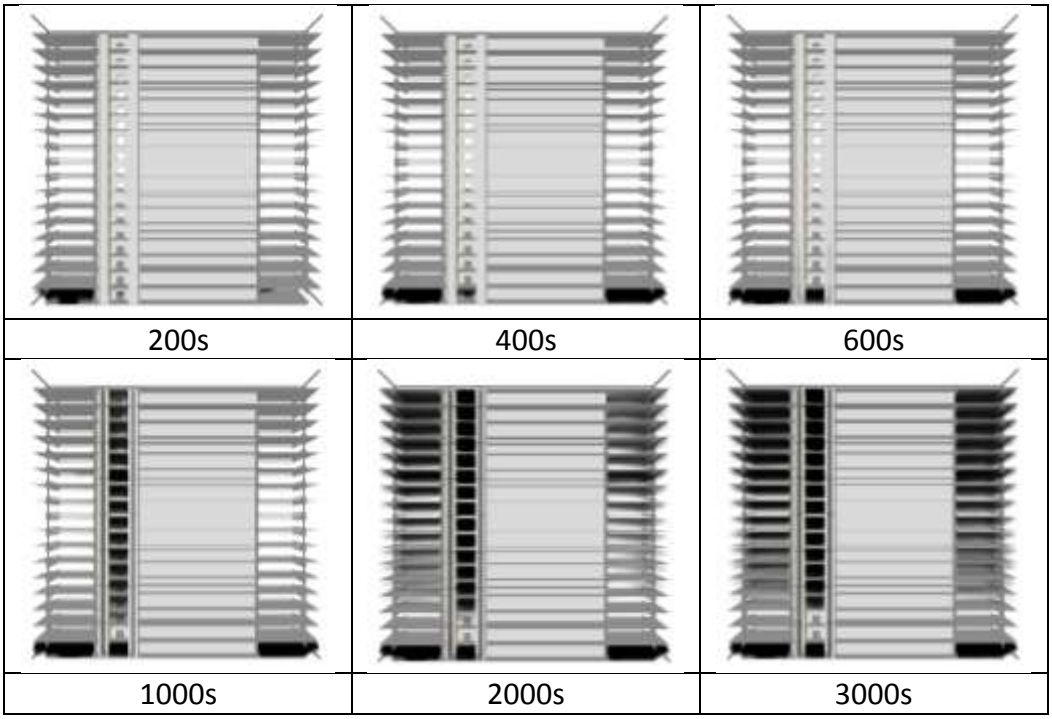

Figure 22 Smoke spread visualization of FO-4 (enclosed with open doors)

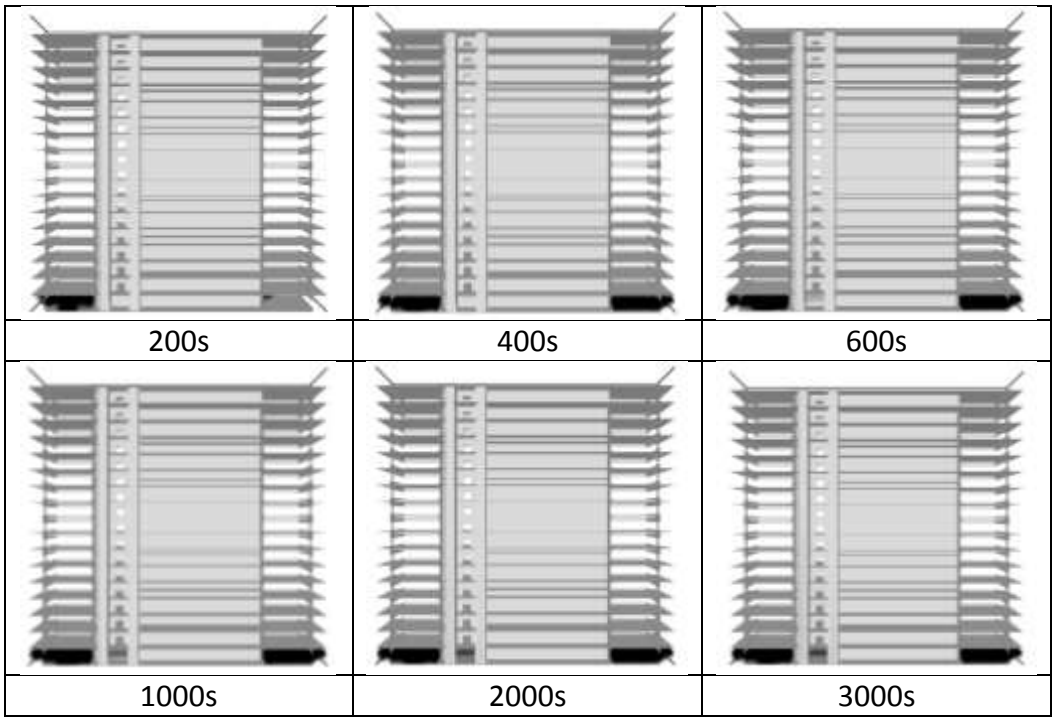

Figure 23 Smoke spread visualization of FO-6 (enclosed with leakage)

Figures 24 and 25 present comparisons of temperature and pressure differences with different enclosure conditions for the elevator lobbies. When the elevator lobbies are enclosed but with open doors, both the steady temperature and pressure differences were reduced significantly. Both the temperature and pressure differences of this case are about 50% of the unenclosed condition. When the elevator lobbies are completely enclosed with a closed door, the temperature and pressure in the elevator shafts are not affected by the fires, and they are both nearly the same as the initial values.

From Figure 25, we also find that the neutral plane for the enclosed case is higher than the unenclosed case.

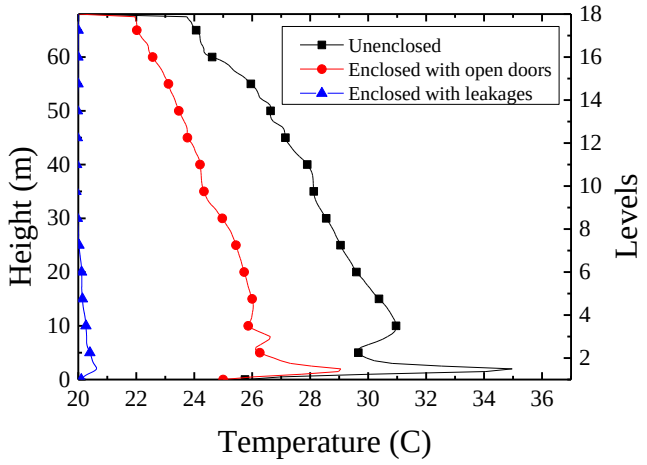

Figure 24 Comparison of steady temperature with different enclosure conditions (at 2000s)

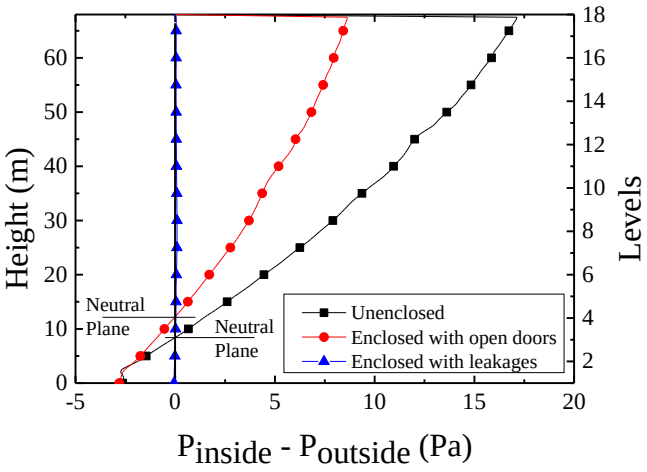

Figure 25 Comparison of steady pressure with different enclosure conditions (at 2000s)

8 FDS simulation with closed elevator doors

Fire simulations with more typical ventilation conditions (closed elevator doors and a typical building envelope) were carried out. First, we considered the fire scenario without temperature difference inside and outside the building (FC1). Then the effect of the typical sealed case and extremes in temperature 9external stack effect) were analyzed in FC2.

Figure 26 and Figure 27 present the temperature slices for cases FC-1 and FC-2. It must be noted that the fires are oxygen/ventilation limited in both cases at about 1800s due to the poor ventilation condition of the building. These transient fire behaviors resulted not only in anunsteady temperature distribution in the elevator shafts, but also in unsteady smoke spread rate through the leakages.

Figure 28 and Figure 29 present the smoke spread visualization of FC-1 and FC-2. In both case, the smoke starts to affect the upper layer at around 600s. Then, significant smoke is observed entering the upper half of the building.

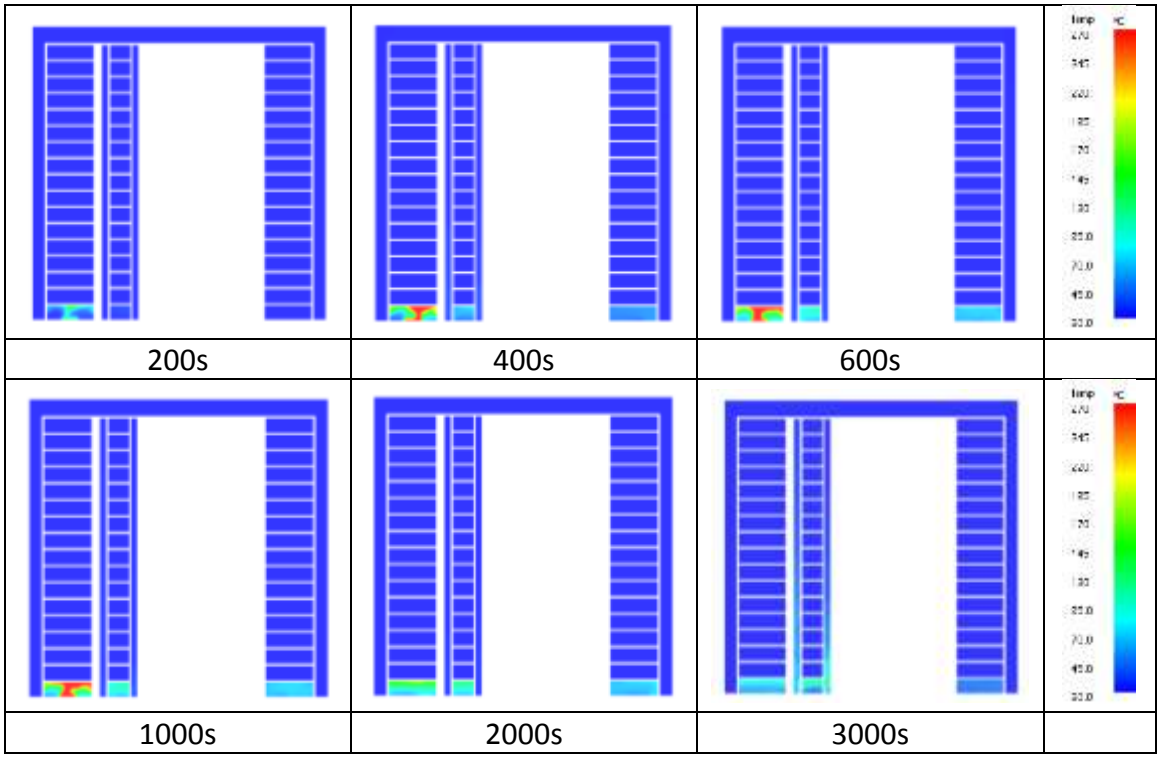

Figure 26 Temperature slice of FC-1

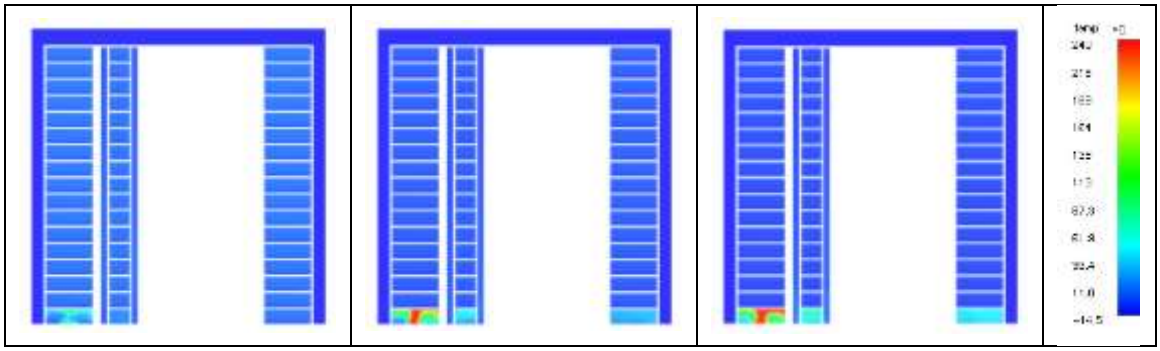

200s	400s	600s	
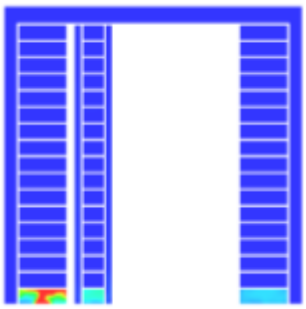	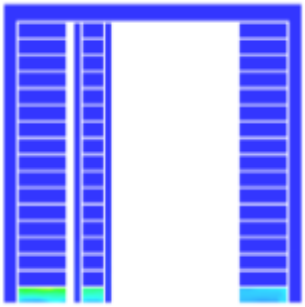	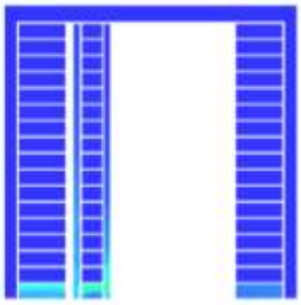	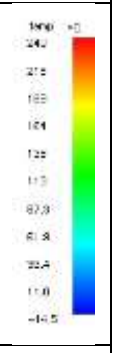
1000s	2000s	3000s	

Figure 27 Temperature slice of FC-2

		
200s	400s	600s
		
1000s	2000s	3000s

Figure 28 Smoke spread visualization of FC-1

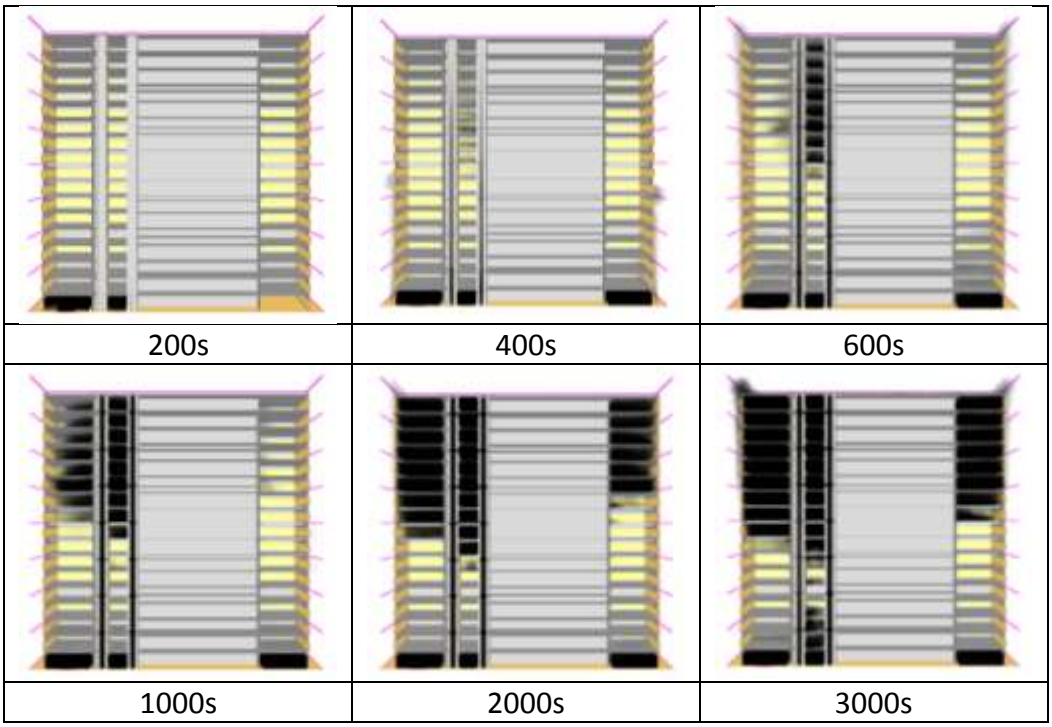

Figure 29 Smoke spread visualization of FC-2

Figure 30 presents the temperature distribution in the elevator shaft for Cases FC-1 and FC-2. For the warm case, the temperatures are all above 20^{o}C due to the heating effect of the fire. However, when it comes to the cold case, the temperature in the shaft keeps decreasing due to the mass exchange with the cold environment. Finally the gas temperature will approach the cold temperature of -15^{o}C on floors below the neutral plane.

Figures 31 and 32 show the pressure distribution in the office area and the shafts, respectively. The pressure profiles show distinct differences between cases FC-1 and FC-2. For case FC-1, both pressure differences (shaft-to-environment and office area-to-environment) increase with time. While in case FC-2, a relatively large initial pressure difference exists due to the initial temperature difference. Due to the stack effect, cold air flows in the building and reduces the temperature and pressure differences. The fire increase in temperature is not as significant as the environmental temperature cooling for some floors.

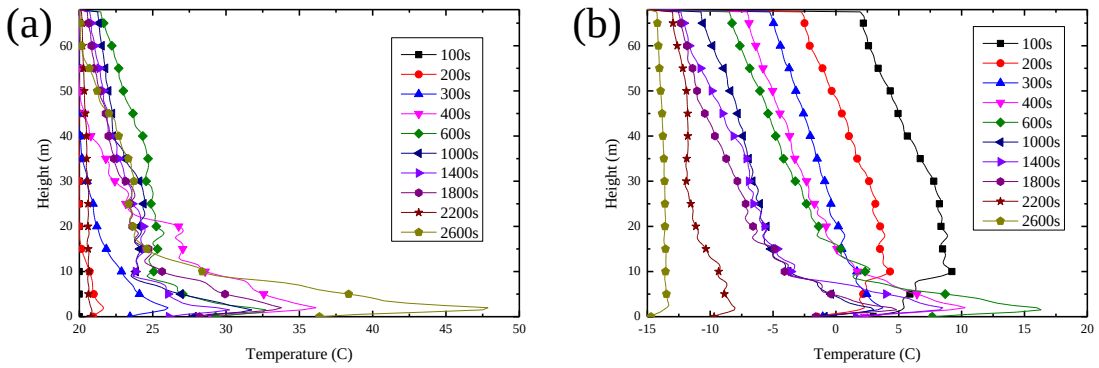

Figure 30 Temperature distribution in the elevator shaft: (a) FC-1 (Warm); (b) FC-2 (Cold)

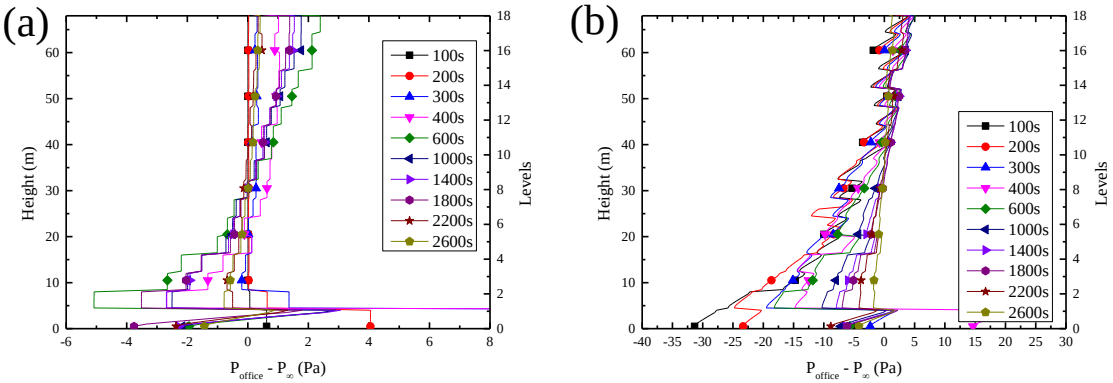

Figure 31 Pressure distribution in office area: (a) FC-1 (Warm); (b) FC-2 (Cold)

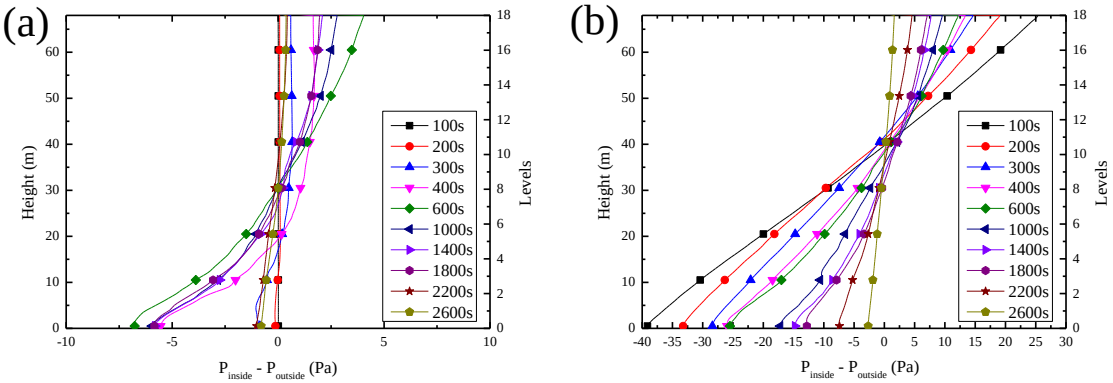

Figure 32 Pressure distribution in elevator shaft: (a) FC-1 (Warm); (b) FC-2 (Cold)

Figure 33 present the mass flow rate through one elevator door on the fire level. For the warm case, the mass flow rate increases for about the first 500s. After that, it gradually decreases. The mass flow rate oscillates a little around 2000s due to the ventilation limitation of the fire. For the cold case, there is an initial mass flow due to the stack effect. The mass flow rate shows generally the same tendency but a bit larger than the warm case.

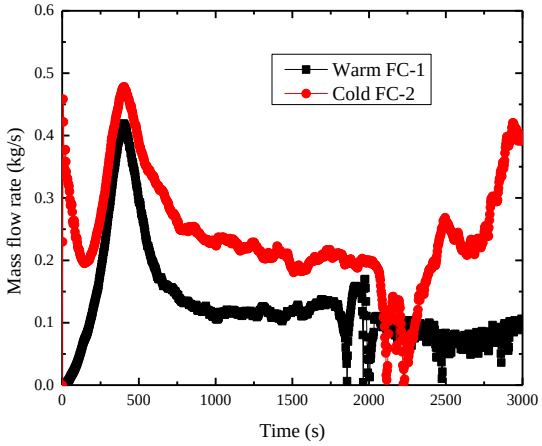

Figure 33 Mass flow rate through the elevator door (Elevator 3) at fire level.

9 Summary of the results

9.1 Safety Criterion

In fires, a major hazard is when potential evacuees are trapped in the early stages of a fire by relatively thin smoke. In some sense, loss of visibility is an indirect but fatal potential hazard. For this reason, a large number of researchers have focused on the relationship between visibility and human behavior [4,18]. A simple visibility model for signs seen through fire smoke is proposed by Jin [20] as

$$V \approx \frac{1}{C_s} In(\frac{B}{\delta_c kL}), \tag{18}$$

where V is the visibility of signs at the obscuration threshold (m), C_s is the smoke extinction coefficient (1/m), B is the brightness of signs (cd/m^2), δ_c is the contrast threshold of signs in smoke at the obscuration threshold (0.01~0.05), k is a coefficient

range from 0.4 to 1.0, and L is $1/\pi$ of mean illuminance of illuminating light from all directions in smoke (1 m/m^2).

It has been found that smoke can reduce occupant walking speed as shown in Figure 34[4]. Other research has indicated that occupants will turn back rather than use an escape route if the visibility in that route is less than approximately 3 meters. For large public buildings it is believed that occupants need to be able to see for at least 10 meters in order to find the escape route[22][23].

Figure 35 presents the typical distribution of the visibility for FO-2. Note that the colorbar range is from 10m to 30m, and the dark red color means the local visibility has dropped below 10m which is unacceptable. We can find that the visibility at upper floors started to decrease at about 600s. At nearly 1000s, significant red regions appear at the 12^{th} floor, which means that it would not be safe for occupants to stay on this floor.

Using the analysis of FO-2, the safety time is defined as the time from fire ignition to the onset of conditions which are hazardous to human occupancy (based on smoke visibility). Table 8 summarizes the safety time for all the cases. When the sprinklers are activated, the fire can be controlled and suppressed, allowing safety times more than 3000s. When the sprinklers fail, only by enclosing the elevator lobby do we get a relatively long safety time.

An evacuation study of this building suggests that the quickest way (using whole occupant evacuation elevators) to evacuate occupants from the building would take more than 2000s[13]. If we further consider a fire detection time and a factor due to the uncertainty of the simulation, a safety time of at least 3000s would be expected.

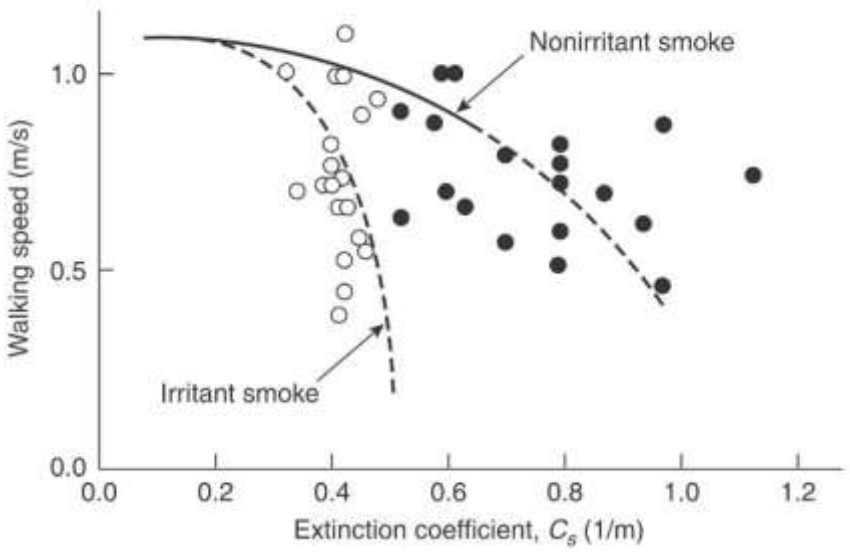

Figure 34 Relationship between the visibility and human behavior[4]

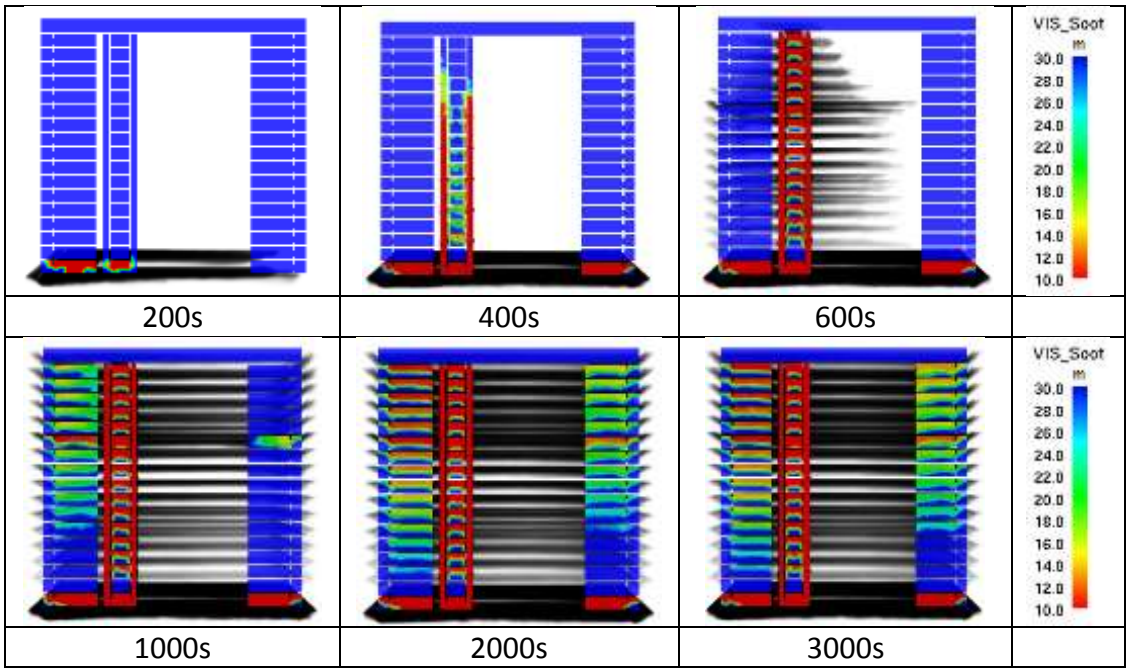

Figure 35 Smoke visibility at section Y=20.5m (the centerline section of elevator 3 and elevator 7) with a 7MW fire located at the first floor (FO-2)

Table 8 Summary of safety time

Case	Windows	Sprinkler	Elevator lobby	Safety time[a]	Unsafe level[b]
FO-1	Closed	Failed	Unenclosed	1362s	12
FO-2	Open	Failed	Unenclosed	936s	12
FO-3	Open	Activated	Unenclosed	>3000s	-
FO-4	Open	Failed	Enclosed with open door	2181s	12
FO-5	Open	Activated	Enclosed with open door	>3000s	-
FO-6	Open	Failed	Enclosed with leakage	>3000s	-
FC-1	Leakages	Failed	Unenclosed	984s	12
FC-2	Leakages	Failed	Unenclosed	1174s	12

a. Safety time indicates the time when the visibility of significant area drops below 10m.
b. Unsafe level indicates the location where the visibility drops below 10m.

9.2 Mass flow rate at fire level

The mass flow rates at elevator door of fire level are summarized in Table 9. When the elevator doors are opened at the fire floor, the mass flow rate caused by the fire is comparable to the case caused by the stack effect in Table 5.

Table 9 Summary of Mass flow rate at elevator door of fire level

Case	Windows	Sprinkler	Elevator lobby	Mass flow rate per shaft
FO-1	Closed	Failed	Unenclosed	2.59 kg/s
FO-2	Open	Failed	Unenclosed	3.32 kg/s
FO-3	Open	Activated	Unenclosed	1.78 kg/s (Maximum)
FO-4	Open	Failed	Enclosed with open door	2.04 kg/s
FO-5	Open	Activated	Enclosed with open door	0.30 kg/s (Maximum)
FO-6	Open	Failed	Enclosed with leakage	0.18 kg/s
FC-1	Leakages	Failed	Unenclosed	0.43 kg/s (Maximum)
FC-2	Leakages	Failed	Unenclosed	0.48 kg/s (Maximum)

10 Conclusion

From the current results, some conclusions can be drawn. Compared with previous research[5][6] which considered post-flashover fires with temperature rise of more than 700^{o}C, this study used a single workstation fire of 7MW, which elevates the gas temperature around the elevator lobby by only about 50^{o} C. Thus the fire hazard examined in this report is much smaller than that proposed by others, and the fire-induced stack effect is also smaller. One effect that has not been considered in previous work is the effect of sprinklers. The effects of sprinklers to control the fire were directly considered in this study.

When sprinklers are normally activated, fires can be quickly controlled and suppressed. After the fire is extinguished on the fire floor, the hot environment of the building maintains the fire-induced stack effect in the elevator shafts and transports the smoke to the upper floors. Generally, however, the smoke is less thick than on the fire floor and gradually dissipates.

For an extreme ventilation condition, when the elevator doors are open at the fire floor, significant smoke moves to the upper floors. For such aa case, the enclosure of the elevator lobbies significantly delays the smoke spread to the upper floors. When the doors on the enclosing walls are open, the gas temperature and pressure differences are almost 50% of the unenclosed conditions. When the elevator lobbies are separated by closed doors with modeled leakage, the fire barely affects the elevator lobbies, and little smoke is transported to the upper floors.

For the extreme ventilation cases when the elevator doors and windows are open on the fire floor, there are two ways to satisfy the visibility-based fire safety criterion. One is by ensuring the functional operation of the sprinklers during fires, and the other is to enclose the elevator lobbies.

When the elevator doors and windows are closed and a normal building envelope leakage area exists, the smoke generated from the fire floor still affects the upper floors. Although the total mass flow rate for these typically-ventilated cases are relatively smaller than for the more open/extreme cases, the smoke concentration is larger and thus the visibility-based safety criterion still indicates a safety problem. Thus, the fire hazard

is nearly the same as the extreme ventilations cases of open windows and elevator doors on the fire floor. The cold weather condition showed a slight increase the fire hazard, but it is not the governing factor.

REFERENCES

[1] Rein G (2013) 9/11 World Trade Center attacks: Lessons in fire safety engineering after the collapse of the towers. Fire technology 49 (3):583-585

[2] Richard G. Gann et al (2005) Reconstruction of the Fires in the World Trade Center Towers. Federal Building and Fire Safety Investigation of the World Trade Center Disaster (NIST NCSTAR 1-5)

[3] Drysdale D (2011) An introduction to fire dynamics. Wiley

[4] Babrauskas V (2002) The SFPE Handbook of Fire Protection Engineering. NFPA, Quincy, MA:1

[5] Klote J H. 2004. Hazards Due to Smoke Migration Through Elevator Shafts–Volume I: Analysis and Discussion. Technical Report. National Fire Protection Research Foundation, Quincy, MA, Report 864-I

[6] Black W (2009) Smoke movement in elevator shafts during a high-rise structural fire. Fire Safety J 44 (2):168-182

[7] Cooper LY (1998) Simulating smoke movement through long vertical shafts in zone-type compartment fire models. Fire Safety J 31 (2):85-99

[8] McGrattan K, Hostikka S, McDermott R, et al (2014) Fire dynamics simulator, user's guide (version 6). National Institute of Standards and Technology, Gaithersburg, Maryland, USA

[9] McGrattan K, Hostikka S, Floyd J E, et al (2014) Fire dynamics simulator, technical reference (version 6), National Institute of Standards and Technology, Gaithersburg, Maryland, USA

[10] R.G. Rehm and H.R. Baum (1978) The Equations of Motion for Thermally Driven, Buoyant Flows. Journal of Research of the NBS, 83:297–308.

[11] R. Gaunt et al. (2000) MELCOR Computer Code Manuals: Reference Manuals Version 1.8.5, Volume 2, Rev. 2. NUREG/CR-6119, US Nuclear Regulatory Commission, Washington, DC, 91

[12] Hamins A, McGrattan K (2003) Reduced-scale experiments on the water suppression of a rack-storage commodity fire for calibration of a CFD fire model. Fire Safety Science 7:457-468

[13] Ronchi E, Nilsson D (2014) Modelling total evacuation strategies for high-rise buildings. Build Simul 7 (1):73-87.

[14] Thomas J. Ohlemiller et al. (2005) Fire Tests of Single Office Workstations. Federal Building and Fire Safety Investigation of the World Trade Center Disaster (NIST NCSTAR 1-5C)

[15] Karlsson B, Quintiere JG (2000) Enclosure fire dynamics. CRC

[16] VanGeyn, M. 1994. Positive Pressure Furnace Fire Tests. Technical Report. National Fire Protection Research Foundation, Quincy, MA, Report 6285

[17] NFPA 2000. Recommended Practice for Smoke Control Systems, NFPA 92A, National Fire Protection Association, Quincy, MA.

[18] Hassan M. Bagheri (2013) ASHRAE Handbook, Fundamentals

[19] Jo J-H, Lim J-H, Song S-Y, Yeo M-S, Kim K-W (2007) Characteristics of pressure distribution and solution to the problems caused by stack effect in high-rise residential buildings. Build Environ 42 (1):263-277

[20] T. Jin, (1978) Visibility through Fire Smoke, J. of Fire & Flammability, 9, pp. 135–157

[21] Stec AA, Hull TR (2010) Fire toxicity. Elsevier

[22] BSI (2004) The application of fire safety engineering priciples to fire safety design of buildings. Human factors. Life safety strategies. Occupant evacuation, behaviour and condition. PD 7974-6:2004

[23] Ramachandran G, Charters D (2011) Quantitative risk assessment in fire safety. Routledge,